5 External-field-driven flow

One of the simplest ways to implement time-dependent boundary conditions in SOMA is to apply a time-dependent external field that is only nonzero close to the boundaries and has the form:

$$E_i(\mathbf{r}) = f_i(\mathbf{r})\phi_i(\mathbf{r})\,, \qquad (5.1)$$

where $i = \mathrm{A}, \mathrm{B}$ denotes the monomer types. In this section, self-assembled lamellae of diblock-copolymers are moved at constant speed v perpendicular to their orientation using spatially periodic external fields close to the boundaries. In a system that moves along with the external field, each monomer experiences a friction force ζv in the opposite direction. This force, which is a consequence of the applied MC scheme to simulate Brownian dynamics, causes the lamellae to bend and eventually tear at high values of v.

5.1 Reference system

A system of $n = 750$ symmetric diblock-copolymers with $N_A = N_B = N/2 = 16$ and $\chi N = 20$ is used. The box dimensions are $L_x \times L_y \times L_z = 2.5 \times 2.82 \times 1\, R_e^3$, which corresponds to $\sqrt{\bar{N}} = 106$. The spatial discretisations are $\Delta x = 1/16\, R_e$, $\Delta y = 47/800\, R_e$ and $\Delta z = 1\, R_e$. To generate the initial lamellar structure, external fields are applied, as shown in Figure 5.1. The interlayer spacing of $d = 1.41\, R_e$ was found to be stable over the duration of the simulations, but it does not correspond to the equilibrium spacing.

Subsequently, the external fields are switched off everywhere except at a distance less than $b = 0.5\, R_e$ from the boundaries in the x-direction, so the length of the part of the lamellae that is not supported by the external fields is $L = 1.5\, R_e$. Every Δt MCS, the fields are moved by a distance of Δy in the y-direction, so the velocity is

$v = 47R_e/(800\Delta t)$. The external fields balance the friction forces at the boundaries and therefore act as bearings for the lamellae.

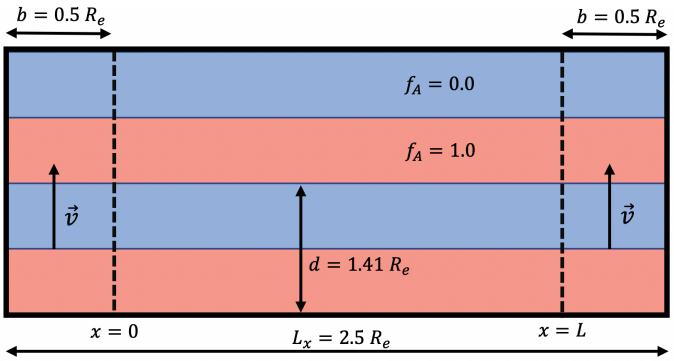

Figure 5.1: Sketch of the external field $f_{\mathrm{A}}(\mathbf{r})$. Red domains correspond to $f_{\mathrm{A}} = 1.0$, blue domains to $f_{\mathrm{A}} = 0.0$. $f_{\mathrm{B}}(\mathbf{r})$ is exactly complementary. Within the region bounded by the dotted lines, the external fields are switched off after the initial lamella structure has been generated.

5.2 Bending modulus

The free energy for a bent monolayer of diblock-copolymers is [25]:

$$F = \frac{1}{2}K\int dx\left(\frac{\partial^2 u}{\partial x^2}\right)^2 \equiv \int dx f(u''), \tag{5.2}$$

where K is the bending modulus and $u \equiv u(x)$ is the deformation profile of the lamella center of mass. The total friction force acting on the monolayer is:

$$F_{fric} = -\rho_0 dLL_z\zeta v = -\frac{nN}{L_xL_y}Ld\zeta v\,, \tag{5.3}$$

where $\rho_0 = nN/V$ is the mean monomer density in the system. The deformation profile can be obtained by solving the following Euler-Lagrange equation:

$$\frac{d^2}{dx^2}\left(\frac{\partial f}{\partial u''}\right) = F_{fric}\,. \tag{5.4}$$

Defining $q \equiv -\frac{nN}{L_xL_y}d\zeta v$, this gives:

$$K\frac{\partial^4 u}{\partial x^4} = q\,. \tag{5.5}$$

With the boundary conditions $u(0) = u(L) = 0$ and $u''(0) = u''(L) = 0$, one obtains:

$$u(x) = \frac{qx}{24K}(L^3 - 2L^2x + x^3)\,, \tag{5.6}$$

in complete analogy to a beam bending under a uniform load q in the Euler-Bernoulli theory. The resulting lamella profile for $v = 0.34R_e/\tau_R$ is shown in Figure 5.2. The fit is in excellent agreement with the simulation data.

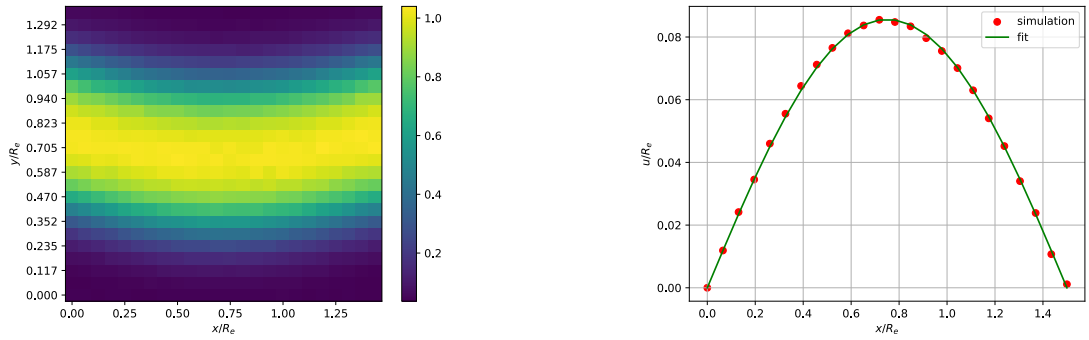

(a) (b)

Figure 5.2: (a) Heatmap of the steady-state lamella profile in the reference frame that moves with the external field, averaged over all lamellae. (b) Lamella center of mass curve for $v = 0.34R_e/\tau_R$. The fit corresponds to (5.6).

The maximum deflection is:

$$u_{max} = u(L/2) = \frac{5qL^4}{384K}\,. \tag{5.7}$$

To obtain the bending modulus, u_{max} is measured for various values of q, this is shown in Figure 5.3. From (5.7), one obtains $K = 39.00\,k_BTR_e$. In equilibrium, it may also be obtained directly from the simulation parameters [25]:

$$K = \frac{3}{16}\left(\frac{12}{\pi^2}\right)^{1/3}\left(\frac{\gamma}{k_BT}\right)^{4/3}\bar{N}^{-1/6}R_e^{5/3}k_BT\,, \tag{5.8}$$

where γ is the interfacial tension. In the strong segregation limit, it reads [21]:

$$\frac{\gamma R_e^2}{\sqrt{N} k_B T} = \sqrt{\frac{\chi N}{6}} \left(1 - \frac{4 \ln 2}{\chi N}\right) . \tag{5.9}$$

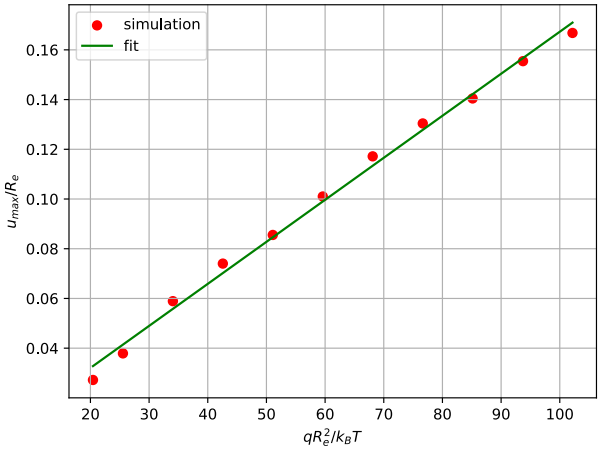

Figure 5.3: Maximum deflection u_{max} as a function of the applied load q. The fit corresponds to (5.7).

The result is $K = 38.94\, k_B T R_e$, in excellent agreement with the simulation results. However, it should be noted that (5.8) is derived from the equilibrium spacing d_0. For $\chi N = 20$, [25] predicts $d_0 = 1.24\, R_e$, which is too small (**Need some reference value here to cite**). This is likely to indicate that the strong segregation is not fully reached at $\chi N = 20$. Nevertheless, the results might suggest that the bending modulus K only weakly depends on the monolayer tickness.

36(24):9237–9248, 12 2003. doi: 10.1021/ma030201y. URL https://doi.org/10.1021/ma030201y.

[8] I Ya Erukhimovich and AN Semenov. Nonexponential density relaxation and the dynamic form-factor of polymer melts in the reptation regime. *Zh. Eksp. Teor. Fiz*, 63:275, 1986.

[9] Paul J. Flory. Thermodynamics of high polymer solutions. *The Journal of Chemical Physics*, 10(1):51–61, 1942. doi: 10.1063/1.1723621. URL https://doi.org/10.1063/1.1723621.

[10] J. G. E. M. Fraaije, B. A. C. van Vlimmeren, N. M. Maurits, M. Postma, O. A. Evers, C. Hoffmann, P. Altevogt, and G. Goldbeck-Wood. The dynamic mean-field density functional method and its application to the mesoscopic dynamics of quenched block copolymer melts. *The Journal of Chemical Physics*, 106(10): 4260–4269, 1997. doi: 10.1063/1.473129. URL https://doi.org/10.1063/1.473129.

[11] Ludwik Leibler. Theory of microphase separation in block copolymers. *Macromolecules*, 13(6):1602–1617, 1980.

[12] R.H. Colby M. Rubinstein. *Polymer Physics*. Oxford University Press, 2003.

[13] M. Müller and G. Gompper. Elastic properties of polymer interfaces: Aggregation of pure diblock, mixed diblock, and triblock copolymers. *Phys. Rev. E*, 66:041805, Oct 2002. doi: 10.1103/PhysRevE.66.041805. URL https://link.aps.org/doi/10.1103/PhysRevE.66.041805.

[14] Marcus Müller. Studying amphiphilic self-assembly with soft coarse-grained models. *Journal of Statistical Physics*, 145:967–1016, 11 2011. doi: 10.1007/s10955-011-0302-z.

[15] C. Pangali, M. Rao, and B.J. Berne. On a novel monte carlo scheme for simulating water and aqueous solutions. *Chemical Physics Letters*, 55(3): 413–417, 1978. ISSN 0009-2614. doi: https://doi.org/10.1016/0009-2614(78)84003-2. URL https://www.sciencedirect.com/science/article/pii/0009261478840032.

[16] Shuanhu Qi and Friederike Schmid. Hybrid particle-continuum simulations coupling brownian dynamics and local dynamic density functional theory. *Soft*

Matter, 13:7938–7947, 2017. doi: 10.1039/C7SM01749A. URL http://dx.doi.org/10.1039/C7SM01749A.

[17] Ellen Reister. *Zusammenhang zwischen der Einzelkettendynamik und der Dynamik von Konzentrationsfluktuationen in mehrkomponentigen Polymersystemen*. PhD thesis, Mainz, 2002.

[18] Peter J. Rossky, Jimmie D. Doll, and Harold L. Friedman. Brownian dynamics as smart monte carlo simulation. *Journal of Chemical Physics*, 69:4628–4633, 1978.

[19] Prince E. Rouse. A theory of the linear viscoelastic properties of dilute solutions of coiling polymers. *The Journal of Chemical Physics*, 21(7):1272–1280, 1953. doi: 10.1063/1.1699180. URL https://doi.org/10.1063/1.1699180.

[20] Ludwig Schneider and Marcus Müller. Multi-Architecture Monte-Carlo (MC) Simulation of Soft Coarse-Grained Polymeric Materials: SOft coarse grained Monte-carlo Acceleration (SOMA). *arXiv e-prints*, art. arXiv:1711.03828, November 2017. doi: 10.48550/arXiv.1711.03828.

[21] A. Semenov. Theory of Long-Range Interactions in Polymer Systems. *Journal de Physique II*, 6(12):1759–1780, 1996. doi: 10.1051/jp2:1996159. URL https://hal.science/jpa-00248405.

[22] A. N. Semenov. Theory of Long-Range Interactions in Polymer Systems. *J. Phys. II*, 6(12):1759–1780, December 1996. ISSN 1155-4312. doi: 10.1051/jp2:1996159.

[23] Jörn Ilja Siepmann and Daan Frenkel. Configurational bias monte carlo: a new sampling scheme for flexible chains. *Molecular Physics*, 75(1):59–70, 1992. doi: 10.1080/00268979200100061. URL https://doi.org/10.1080/00268979200100061.

[24] Glenn M. Torrie and John P. Valleau. Monte carlo free energy estimates using non-boltzmann sampling: Application to the sub-critical lennard-jones fluid. *Chemical Physics Letters*, 28(4):578–581, 1974. ISSN 0009-2614. doi: https://doi.org/10.1016/0009-2614(74)80109-0. URL https://www.sciencedirect.com/science/article/pii/0009261474801090.

[25] Z.-G. Wang and S.A. Safran. *J. Phys. (Paris)*, 51:185, 1990.